euronoise

Improvement of the GMM-AR classification of multiframe contrast ultrasound images using gaussian filter

Bilal Ghazal[a], Maha Khachab[b], Denis Friboulet[c], Chafic Mokbel[b] and Christian Cachard[c]

[a]Univ. of Balamand Lebanon and Univ. of Claude Bernard France, Main Road Abdel Halim Ghazal bldg Kab-Elias Bekaa, 00961 Kab-elias, Lebanon
[b]Univ. of Balamand, Biomedical Dept., El Koura, 00961 Tripoli, Lebanon
[c]Université de Lyon, 43 boulevard du 11 Novembre 1918, 69622 Villeurbanne, France
bilalghazal00@hotmail.com

Speckle noise constitutes the main drawback of ultrasound images. Despite the use of contrast agents that enhance the visualization of vascular zones, the backscattered signals from the contrast agent and tissue are still close which prevents a wide use of contrast agent for diagnosis. Thus, it was necessary to implement image-processing techniques that enhance the contrast echo and have the capability of classification. We have applied a new approach based on the autoregressive model where an image of prediction errors is calculated in the first phase. Then, a Gaussian filter is applied to the prediction error distribution before classification by a Gaussian mixture model. The Agent to Tissue Ratio (ATR) factor and Fisher criterion are adopted to compare the performance of this method with harmonic and B mode images. These experiments show the advantages of our proposed approach.

1 Introduction

Echography is cheap, simple and safe, operates with low cost, and does not need heavy equipments. Its importance has increased recently with the introduction of ultrasound contrast agents and the implementation of newer image-processing techniques. Moreover, the ultrasound scanner visualizes organs and blood vessels and is commonly used by medical professionals as a diagnostic tool. We are mainly interested in cardiac contrast-agent applications and specifically the discrimination between the perfused zone and the surrounding tissue. This discrimination yields critical information about blood perfusion of the heart and blood flow rate, information that actually assesses heart function. Contrast agents injected intravenously increase the performance of ultrasound images. Their small diameter of 1-10 μm prevents their total destruction by pulmonary capillaries and allows them to reach cardiac cavities. Because they are formed by air or gas bubbles, they are frequently protected by encapsulated surfactant shell to resist the high pressure in the cardiac cavities [1]. In addition, the density and the compressibility of these microbubble agents are different from those of the blood and surrounding tissues causing an enhancement of the backscattered signals. Moreover, because of their nonlinear behavior, contrast agents generate harmonics, subharmonics, and ultraharmonics of the incident ultrasound waves. This leads to several ultrasound-imaging modes [2-5] based upon the nonlinear component of the signal [8]. We have previously applied the autoregressive (AR) model [6,9] on the backscattered signal to separate the tissue part and the agent part, and we have also applied the Gaussian mixture model (GMM) combined to the AR model to achieve a good classification. This consisted of introducing two Gaussian-functions mixture to model autoregressive-prediction errors associated to tissue and contrast agent, so that a contrast enhancement between these two partitions can be accomplished. In this paper, we propose to implement a new variant approach that improves the contrast images classification by means of the GMM-AR technique. The approach consists of applying a Gaussian filter as an intermediary step before applying the GMM classifier and after establishing the image of prediction errors using AR-covariance method [6]. Our results have shown that the prediction error is relatively large for the signal issued from contrast agents when compared to that from the tissues. As noted in [11] this filtering step makes the prediction error distribution closer to a Gaussian distribution. The GMM then models the modified distributions into two partitions according to the filtered prediction-error image pixel values. This new variant approach shows a better performance than that of the existing techniques and the harmonic mode [4] that is being implemented in most ultrasound scanners.

2 Multiframe classification using modified GMM-AR technique

The acquired RF frames are of a three-dimensional data volume (2D + time) composed of F frames as shown in Figure 1. Every frame is a 2-dimensional B mode image made of L RF signals. The RF signal represents the backscattered echoes involving the depth information. It is assumed that the points of coordinate (i,j) from each frame belong effectively to the same scatterer and that the displacement effect due to motion is negligible. We define an acquisition vector X_{ij} consisting of N (N<=F) points (i,j) that are located into the consecutive frames as shown in Figure 1.

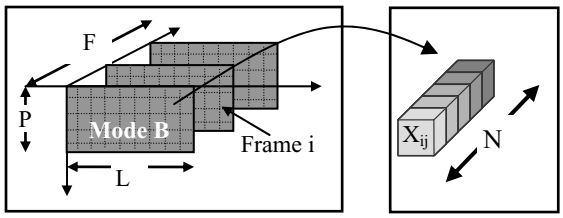

Figure 1: left: Data volume 2D + time consisting of F frames where each frame is a B mode image formed by L lines and P points. Right: zoom of an X_{ij} vector constituted by N consecutive pixels deriving from the same position (i,j).

The AR-based method is applied to each vector, so that the linear/nonlinear behavior of the scatterer is expressed. For a tissue scatterer, the prediction error is assumed to be low, while for the agent, it is relatively high. The AR-based covariance method is selected in this approach to calculate the prediction error, since it has been shown to be the best method among the other AR-based techniques [6].

2.1 Autoregressive covariance method

The autoregressive model (AR) uses the assumption of a linear system in order to predict the sample x(n) value based on its previous p samples. The corresponding prediction error is given by:

$$e(n) = x(n) - \hat{x}(n) = \sum_{i=0}^{p} a(i)\, x(n-i) \qquad (1)$$

where *a(i)* are the prediction coefficients calculated using the Levinson-Durbin algorithm [10], $\hat{x}(n)$ is the estimated sample value, and p is the model order.

The covariance method, which is an AR-based approach [6], gathers the adjacent acquisition vectors into rectangular blocks. For a given block, the covariance matrix is calculated in order to determine its associated global AR parameters. Then, the prediction error for the block pixels is locally estimated (1) using these global coefficients, and the prediction-error image is obtained by processing all the image's blocks. Because the tissues' backscattered signal has a linear diffusion characteristic, the covariance method may simulate it and yields a low prediction error. Whereas for the contrast agent, its backscattered non-linear signal is not well modeled by the linear AR model, and the prediction error is relatively greater.

The approach that we have proposed in our previous work [9] consisted of combining the AR-covariance method and the GMM model. The modeling of the prediction error associated with agent and tissues regions by two Gaussians produced satisfying results. However, we can improve this technique, if we ensure that these distributions are close to Gaussian before applying the GMM model.

2.2 Gaussian filter

The GMM models both the contrast and tissue distribution by a Gaussian function. It assumes Gaussian distributed observations. Therefore, we propose to apply a Gaussian filter to the prediction error image in order to have a distribution closer to a Gaussian [11], in agreement with the central limit theorem [12]. This assumption is verified in the results section using a Goodness-Of-Fit (GOFT) test [13].

2.3 Gaussian mixture model

The Gaussian model aims to model a distribution by a Gaussian function characterized by its mean μ_x and its variance σ_x^2. The Gaussian probability density function [12] denoted by $\mathcal{N}(x, \mu_x, \sigma_x^2)$ is given by equation 2.

$$f_X(x) = \frac{1}{\sqrt{2\pi}\sigma_x} \exp\left[-\frac{(x-\mu_x)^2}{2\sigma_x^2}\right] \qquad (2)$$

The Gaussian mixture model combines many density functions possessing different parameters and linearly weighted by w_i (3).

$$F_x = \sum_i^G w_i \mathcal{N}_i(x, \mu_x, \sigma_x^2) \qquad (3)$$

The study of the statistics of the AR prediction error of contrast ultrasound images illustrates the presence of two distribution categories: low values for tissue and relatively high values for agent. Indeed, the prediction error associated to tissue yields a low mean μ_T and a small variance σ_T^2 since the tissue scatterers' response is linear [10] and relatively homogenous. As for the agent distribution, its corresponding mean μ_A is high because the agent's scatterers are nonlinear [14-15]. Moreover, in the blood, the agent dissolution is non-homogeneous and the scatterers' position is randomly disposed which lead to a high variance value σ_A^2. Therefore, the modeling of these two distributions by a GMM model, constituted by two Gaussians $\mathcal{N}(T, \mu_t, \sigma_t^2)$ and $\mathcal{N}(A, \mu_a, \sigma_a^2)$, yields discrimination since the distributions are close to Gaussian and the means take clearly different values.

2.4 Algorithm procedure

Our approach achieves a classification between the contrast agent and tissues. Each iteration is constituted by an AR-covariance pretreatment method, a Gaussian filter stage, then a GMM classifier. An initialization phase is required to determine the initial parameters of the Gaussian and to find out the primary classes pixels set. First, the covariance method is applied and the prediction-error image is established. Second, the initial Gaussians functions are set to have the same mean as the mean whole distribution. As for their covariance, they are equal to the whole distribution covariance weighted respectively by 0.9 and 1.1. A threshold attributes the pixels to the preliminary tissue and agent partitions.

For now, the pixels set are gathered into two groups. The covariance method is globally and separately applied to each group, and two families of prediction error coefficients are determined. To calculate the prediction error image, we combine the probabilities a posteriori P_1 and P_2 and the prediction coefficients a_1 and a_2 as shown in equation (4).

$$\hat{x}(n) = P_1 \sum_{i=1}^{p} a_1(i)\, x(n-i) + P_2 \sum_{i=1}^{p} a_2(i)\, x(n-i) \qquad (4)$$

Next, the Gaussian filter is applied to the image followed by a GMM that aims to classify the pixels into two classes by means of maximum likelihoods. At each iteration, new model parameters values are calculated, and the pixels are reattributed again towards the contrast and tissue classes. Applying Gaussian's filter at each iteration yields the adaptation of the GMM with the image complexity and feature. In addition, it allows a progressive localization of the contrast zone and a gradual determination of the separation contour.

3 Experimental setup

A tissue phantom consisting of a synthetic material having acoustic properties similar to biological tissues (backscattered ratio 10^{-4} [1/cm/sr], attenuation 1.5 dB/cm for a scanned frequency 2.25 MHz) has been used. The contrast agent used is SonoVue™ [14] which belongs to the second generation of agents conceived by Bracco Research (Geneva). The microbubbles are hexafluoride sulfide gases (SF_6) stabilized by a phospholipid shell. The phantom is immerged in a tank containing 800 ml of NaCl (0,9%) solution. This solution is diluted by adding an initial dose of agents using a micropipette. A magnetic stirrer is used to keep the solution in the tank in circulation. The ultrasound beam of 2.5 MHz fundamental frequency traverses 38 mm in the phantom before reaching the agent zone. The ultrasonic acquisition system is a MEGAS echography connected on one hand to the PA230E probe and on the other hand to an acquisition system for processing RF signals called platform FEMMINA [15-16]. The acquired

data volume is formed by 50 images where each image is composed of 80 lines that cover an exploration sector of 75 degrees. Each RF signal is constituted by 3117 pixels and probes a depth of 6 cm. To construct the B mode image, the RF signal is demodulated by envelope detection operator then is displayed on Cartesian coordinates by axes transformation from the polar coordinates.

The calculation of the AR parameters requires the observation of a sequence of N samples ($N > p$) from the signal. This requires the observation of N consecutive frames since the dimension of the X_{ij} vectors is equal to the number of samples. Unfortunately, the cardiac motion constrains the number of frames that can be used. The cardiac rate varies from 70 up to 200 beats/min depending on the patient. The echographic frames' frequency is in the range of 10 to 60 Hz. This limits the number of frames to process from 10 to 50 frames. Since the frame rate is 33 Hz, we propose to select five consecutive frames to reduce the influence of the movement and to have enough frames to apply the model.

4 Results

The second phase of each algorithm's iteration is divided into two steps. The first consists of applying the Gaussian filter to ensure that the tissues and contrast agent distributions are close to Gaussian. In the second step, GMM is used to model these distributions.

To evaluate quantitatively the Gaussian assumption, we propose to use a Goodness-Of-Fit measure. GOFT is calculated as the root mean squared error (rmse) between the best Gaussian function that fits the histograms bins and the interpolation function constituted by the bins' center [13].

In fact, in order to observe clearly the role of the Gaussian filter before exposing our results, we choose to apply successively to the first prediction-error image a Gaussian filter and to study the evolution of the GOFT parameter. The associated GOFT values are depicted in Table 1. The results show that GOFT values decrease and that the distributions correspond to the Gaussian shape after Gaussian filter application.

Iteration	GOFT
1	0.0048
2	0.0045
3	0.0043
4	0.0042
5	0.0041

Table 1: Values of GOFT parameter after applying successively a Gaussian filter on the first prediction-error image

On the other hand, Figure 2 illustrates the corresponding distribution obtained for the prediction-error corresponding to the first iteration, when one to five Gaussian filtering steps are applied. Since we aim to express the Gaussian observations, we present at different scales the histograms of tissue agent, about 8000 and 25000 respectively. The green curve is the shape of the GMM Gaussian functions that characterizes the model. This curve proves, in both tissue and contrast cases, how their distributions fit Gaussian model and how they gradually tend to a Gaussian.

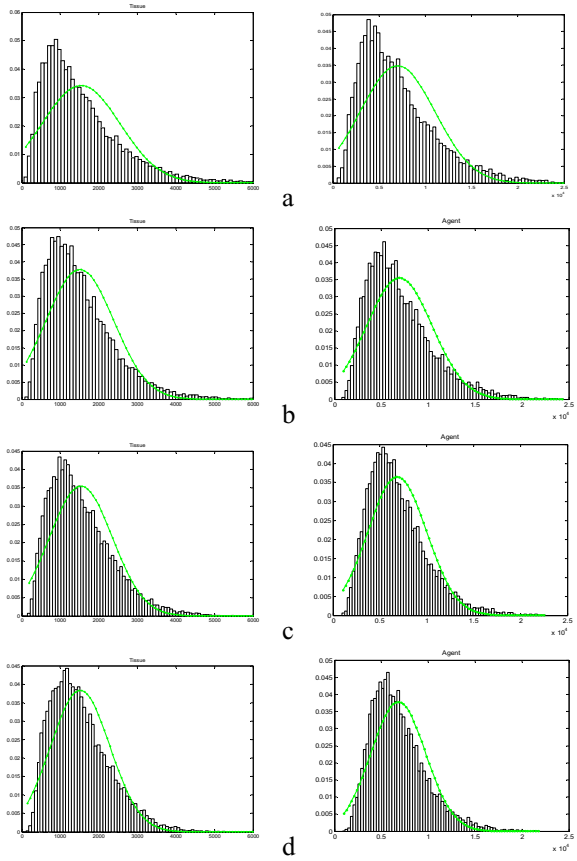

Figure 2: distributions of tissue (left) and contrast agent (right) for the first obtained prediction-error image a) and filtered by a Gaussian filter one b), two c) and three d) times. Tissue scale is about 8000 while the agent scale is 25000.

Moreover, the Fisher criterion may give an idea about the classification feasibility capability when applying the Gaussian filters. Table 2 shows that the Fisher criterion increases gradually for the first six iterations, and thus the classification feasibility raises progressively.

Iteration	1	2	3	4	5	6
Fisher	0.97	1.31	1.55	1.72	1.92	2.01

Table 2: Value of Fisher criterion for the first six iterations. It is clear that Fisher increases gradually.

It is obvious that our proposed approach that introduces the Gaussian filter yields better results than those in the previous approach or the B mode technique. The visualization of the prediction-error image is given in Figure 3. It may be observed that the Gaussian filtering (Figure 3c) yields an improvement as compared to the unfiltered prediction error image (Figure 3b) or the B mode image (Figure 3a).

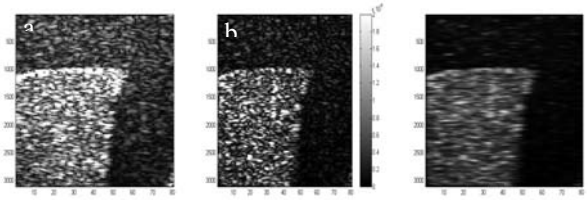

Figure 3: a) B mode image. b) Image prediction error after applying the AR-covariance method c) image prediction error filtered by a Gaussian filter.

The quantitative comparison of the performance of these images may be made using two parameters. The Agent to Tissue Ratio (ATR) (5) is frequently used [17] in the ultrasonic imaging modes to compare the methods efficiency. Since the second phase of the algorithm is the discrimination between tissue and agent, a statistical parameter based on mean and standard deviation as Fisher criterion (6) is adopted in order to evaluate the classification feasibility. These two parameters are calculated inside two identical windows of a dimension of 50 points x 10 lines which are located at the same depth in tissues and contrast agent regions respectively. Theses parameters are defined as:

$$ATR = 20\log_{10}\left(\frac{\mu_a^w}{\mu_t^w}\right) \quad (5)$$

$$FISHER = \frac{\left|\mu_a^w - \mu_t^w\right|}{\sigma_a^w + \sigma_t^w} \quad (6)$$

where the superscript index w indicates that the parameters μ and σ are calculated according to the windows values.

Table 3 provides the values of these parameters for the various imaging methods. The proposed method (GMM-AR model with Gaussian filter) provides an improvement with respect to the previous approach (GMM-AR model), the B mode and the harmonic images. It yields a better ATR value of 19.20 dB, whereas it is 14.58 dB when we do not introduce the Gaussian filter. In the standard ultrasonic modes as B mode and harmonic mode, the ATR values are 9.50 and 12.13 dB respectively, which are smaller than the ATR associated with the proposed approach.

Methods	ATR factor	Fisher criterion
B mode	9.50	0.97
Harmonic mode	12.13	1.00
GMM-AR model	14.58	0.94
GMM-AR model with Gaussian filter	19.20	2.01

Table 3: Values of ATR factor and Fisher criterion that are obtained for our approach and for the other techniques.

Moreover, the Fisher value (2.01) shows that our approach provides a better discrimination, since this criterion illustrates the overlapping ratio between the two partitions. Figure 4 provides the final classification results and shows that our technique yields better results than those in the existing and previous methods (Figure 4a).

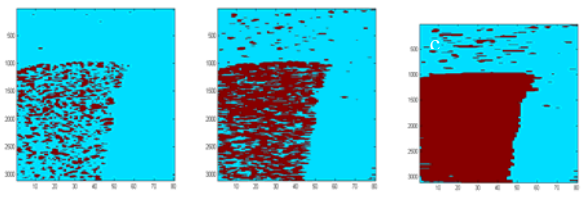

Figure 4: Image classification using AR method coupled to GMM model a), using our approach b), and after applying the erosion dilation as a post treatment technique c).

Figure 4b shows that the classification method yields a good differentiation between the tissues and the vascular zones. At the separation edges, the boundary is not clear, because there is an overlap between agent and tissue areas. To compensate for this drawback, we could apply the erosion dilation technique (Figure 4c).

5 Conclusion and discussions

We have proposed a new approach for enhancing the contrast in ultrasound images with contrast agents. The application of AR-covariance method on multi frame signals provides a prediction-error that has two categories of values, a low prediction error in the case of the tissue and a high prediction error in the case of the contrast agent. This leads to a good separation and contrast enhancement. A Gaussian filter is then applied to improve the modeling of the prediction error distribution for both agent and tissue regions by the GMM model. We have shown that the obtained results are better than those of the harmonic and B mode techniques. By using many classes, we think we could improve the performance of this method and we may quantify the amount of contrast agent in the circulation. A Further interest of the proposed approach relies on the fact that it needs a limited number of frames (five in the present study) which potentially makes it less sensitive to artifact linked to the cardiac motion.

Acknowledgements

We would like to thank the Bracco Research society Geneva for the radio frequency database.

We are graceful to the AUF (Agence Universitaire de la Francophonie) grant for supporting this work.

6 References

[1] De Goertz et all, “The effect of bubble size on nonlinear scattering from microbubbles at high frequencies,” *IEEE Ultrasonics symp*, pp. 1503-1506, 2003.

[2] F. Forsberg, W. Shi et all, “Implementation of subharmonic imaging,” *IEEE Ultrasonics symp*, pp. 1673-1676, 1999.

[3] P. Palanchon, A. Bouakaz et all, “Subharmonic and ultraharmonic emissions for emboli detection and characterization,” *Ultrasound Med. Biol.*, vol. 29, no. 3, pp. 417-425, 2003.

[4] N. Jong, A. Bouakaz and P. Frinking, "Harmonic imaging for ultrasound contrast agents," *IEEE Ultrasonics symp*, pp. 1869-1876, 2000.

[5] P. Shanker, P. Krishna and L. Newhouse, “Subharmonic backscattering from ultrasound contrast agent,” *J. Acoust. Soc. Am.* Vol. 106, no. 4, pp. 2104-2100, Oct, 1999.

[6] B. Ghazal, C. Cachard, et all, "Autoregressive modeling application for vascular zone detection in the

contrast echographic image," *IEEE symp for signal and its application*, Feb, 2007.

[7] W. Law, A. Frizzell, et all, "Determination of the nonlinearity parameter B/A of biological media," *Ultrasound in Med. Biol.,* vol. 11, no. 2, pp.307-318, 1985.

[8] V. Sobros et all, "Contrast agent stability: a continuous B mode imaging approach," *Ultrasound in Med. Biol.,* vol. 23, no.10, pp.1367-1377, 2001.

[9] B. Ghazal, M. Khachab, et all, "Classification of contrast ultrasound images using autoregressive model coupled to Gaussian mixture model," *IEEE Engineering in Medecine and Biology Society*, Aug, 2007.

[10] KaySM, "Modern spectral Estimation: theory and application," *Prentice Hall, Englewood Cliffs*, Nj, 1988.

[11] N. Lin, W. Yu, and J.S, Duncan, "Combinative Multi-Scale Level Set Framework for Echocardiographic Image Segmentation. Medical Image Analysis, 2003, vol. 7, n° 4, p. 529-537.

[12] S. vaseghi, "Advance digital signal processing and noise reduction", *John Willey &Ssons*, second edition 2000.

[13] I. Narsky, "Goodness of fit: what do we really want to know?," *Phys. Stat.*, pp. 70-74, 2003.

[14] D. Bokor, Diagnostic efficacy of SonoVue™, " *The American Journal of Cardiology*, vol. 86, no. 4, pp. 119-124, 2000.

[15] N. Rognin, "Outils de simulation et de quantification en imagerie de contraste échographique", *thèse, Creatis-Université de Lyon1*, 2002.

[16] B. Durning, N. Rognin, C. Cachard, "Ultrasound signals and images simulation of phantoms with contrast agent," *IEEE. Trans. Ultrason. Ferroelect. Freq. Contr*., pp 1710-1713, 2001

[17] A. Bouakaz, N. De Jong, C. Cachard, "Standard properties of ultrasound contrast agent," *Ultrasound in Med. Biol*., vol.24, no.3, pp.469-472, 1998.